Electronic Supplementary Material (ESI) for CrystEngComm.
This journal is © The Royal Society of Chemistry 2017

The impact of *N*,*N*'-ditopic ligand length and geometry on the structures of zinc-based mixed-linker metal-organic frameworks

Andrew D. Burrows, Siobhan Chan, William J. Gee, Mary F. Mahon, Christopher Richardson, Viorica M. Sebestyen, Domenyk Turski and Mark R. Warren

1. General experimental details

All chemicals were sourced from commercial suppliers and used as obtained.

Powder X-ray diffraction patterns were recorded on a Bruker AXS D8 Advance diffractometer at 298 K with copper Kα radiation of wavelength 1.5406 Å. Samples were placed in 0.3 – 0.7 mm diameter Lindemann capillaries, and measured with a 2θ range of 3 – 60°. The step size was 0.02° with time per step of 1.00s. Simulated X-ray powder patterns were generated from single crystal data that were imported into PowderCell.[S1]

Microanalysis data were recorded on a CE-440 Elemental Analyser by Mr Alan Carver at the University of Bath or by the Science Centre at London Metropolitan University. TGA experiments were performed on a Perkin Elmer TGA 4000 Thermogravimetric Analyser. Unless stated otherwise, the samples were heated from 25 °C to 600 °C at 10 °C min^{-1} under a flow of nitrogen (20 cm^3 min^{-1}).

^{1}H NMR spectra were recorded at 298 K on a Bruker Ultrashield 300 MHz spectrometer.

Cambridge Structural Database searches were carried out with Version 5.38 of the database, using ConQuest.[S2] Hits containing additional carboxylate groups as substituents were manually excluded.

2. Synthesis of 3,5-bis(4-pyridyl)-1*H*-pyrazole (Hdpp)

4-Acetylpyridine (11.9 mL, 107.31 mmol) and methylisonicotinate (14.72 g, 107.31 mmol) were both placed in a 500 cm^3 round bottomed flask and stirred vigorously with a large stirrer bar. KO^{t}Bu (12.04 g, 107.31 mmol) was added and a reflux condenser immediately attached. The reaction initiated after approximately five seconds and the solution began to turn into a brown solid, hence grinding of KO^{t}Bu was required. Once cooled the solid was dissolved in water (300 cm^3) and the product was precipitated by the dropwise addition of acetic acid, until the pH was 4-5. The solid was then separated by filtration and washed with water (2 × 50 cm^3) and purified by recrystallisation in the minimum amount of ethanol and water (1:1 mixture). This yielded 3-hydroxy-1,3-di(pyridin-4-yl)prop-2-en-1-one as a white material which was dried at 85 °C for 3 hours. Yield 8.49 g (35 %). ^{1}H NMR (300 MHz, $CDCl_3$): δ/ppm 16.10 (s, 1H, OH), 8.77 (d, 2H), 8.76 (d, 2H), 7.73 (d, 2H), 7.72 (d, 2H), 6.82 (s, 1H).

3-Hydroxy-1,3-di(pyridin-4-yl)prop-2-en-1-one (5.50 g, 24.4 mmol), hydrazine dihydrochloride (2.92 g, 27.8 mmol) and NaOH (1.60 g, 40 mmol) were placed in a 500 cm^3 round bottomed flask and ethanol (80 cm^3) added. The reaction mixture was stirred vigorously for 5 min until a suspension had formed and then heated at reflux overnight. The solvent was removed under reduced pressure, and water (300 cm^3) was added before neutralisation with $NaHCO_3$ (5.0 g). The resultant white solid was separated by filtration, washed with water (2 × 50 cm^3) and air dried. Yield 5.32 g (98 %). ^{1}H NMR (300 MHz, DMSO-d_6): δ/ppm 13.99 (broad s, 1H, NH), 8.64 (d, 4H), 7.79 (d, 4H), 7.61 (s, 1H).

3. Powder X-ray diffraction studies

The powder X-ray diffraction patterns for **1-5** are provided in Figures S1-5, together with those simulated from the X-ray crystal structures.

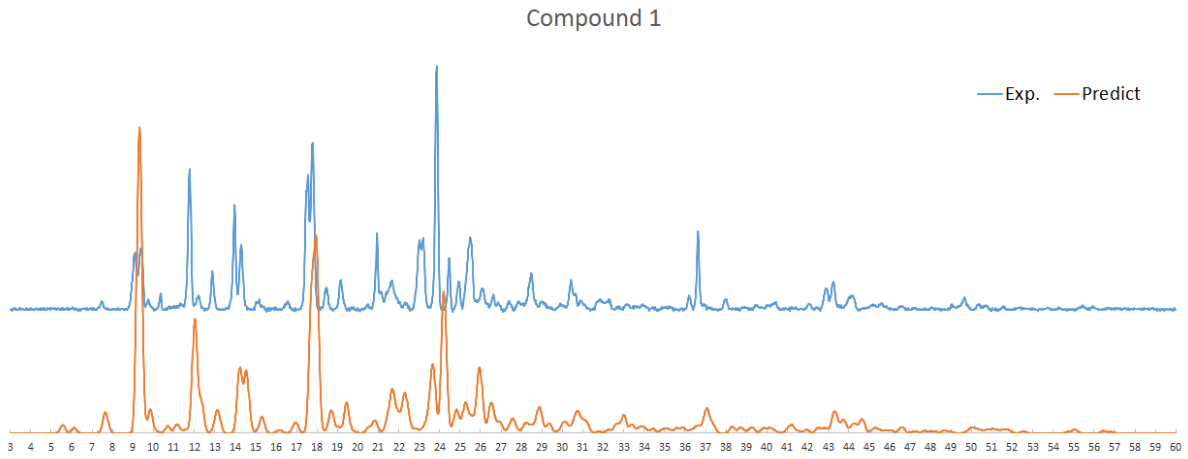

Figure S1. The PXRD pattern for $[Zn_2(bdc)_2(Hdpp)_2]\cdot 2DMF$ **1**, comparing the experimental pattern (top) with that simulated from the X-ray crystal structure (bottom).

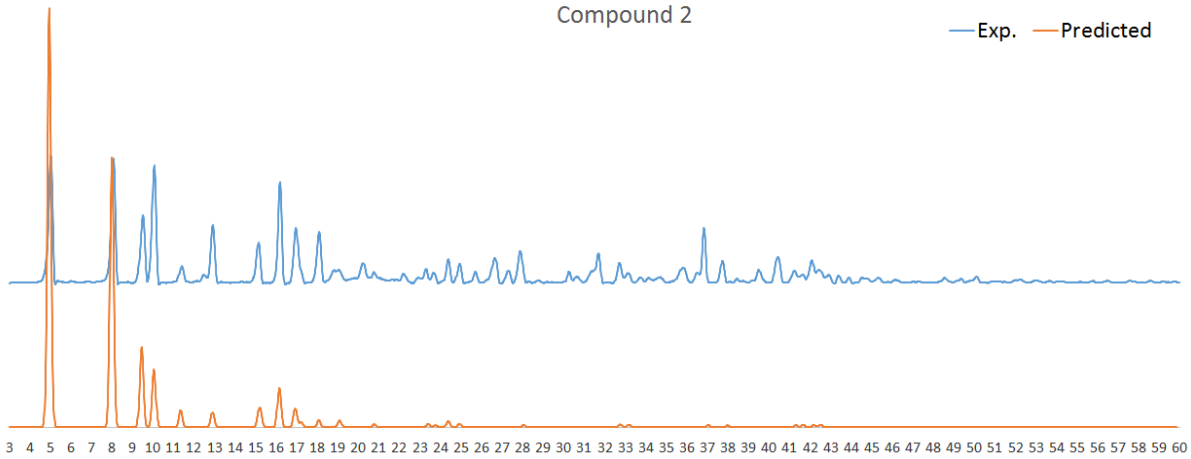

Figure S2(a). The PXRD pattern for the product from the reaction between $Zn(NO_3)_2\cdot 6H_2O$, H_2ndc-1,4 and Hdpp (**2a** and **2b**), in comparison to that simulated from the X-ray crystal structure of **2a**.

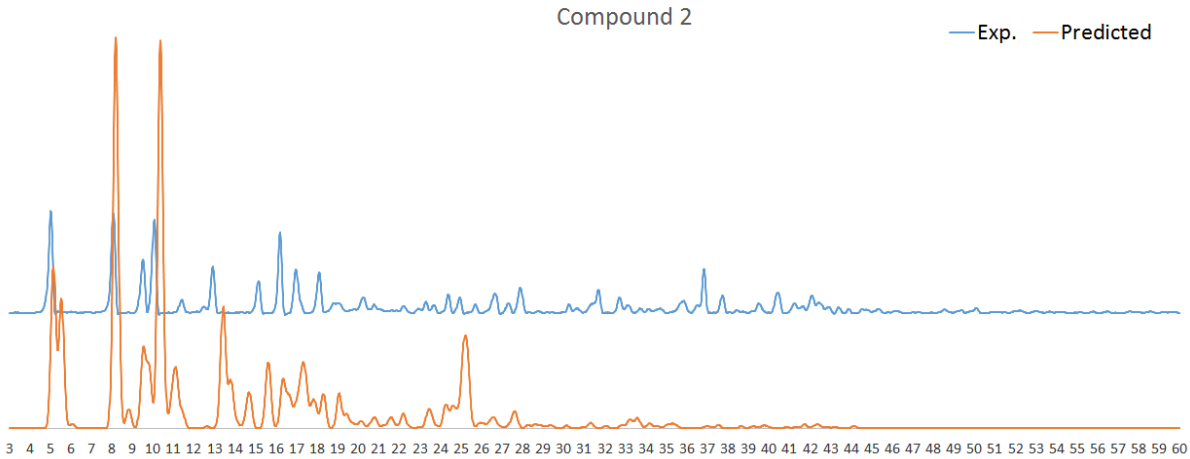

Figure S2(b) The PXRD pattern for the product from the reaction between $Zn(NO_3)_2 \cdot 6H_2O$, H_2ndc-1,4 and Hdpp (**2a** and **2b**), in comparison to that simulated from the X-ray crystal structure of **2b**.

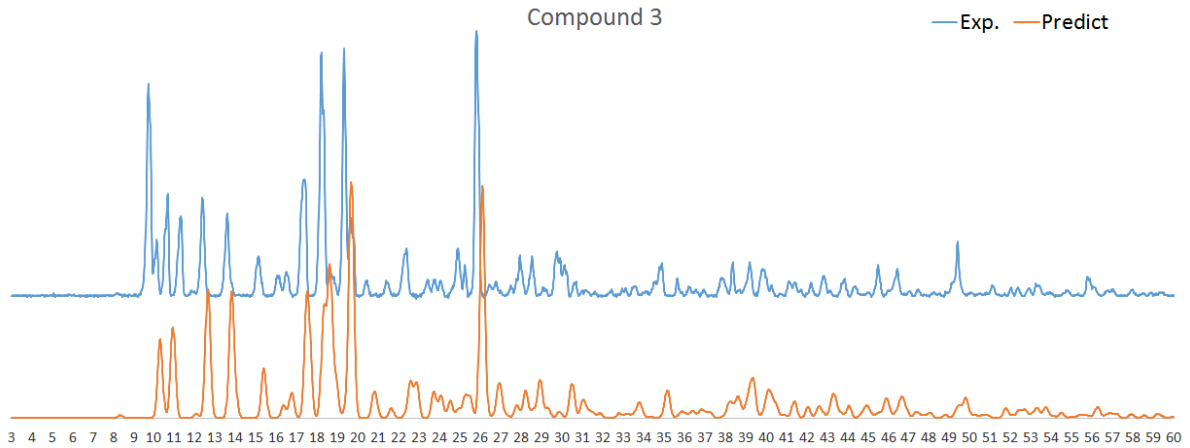

Figure S3. The PXRD pattern for [Zn(mbdc)(Hdpp)]·DMF **3**, comparing the experimental pattern (top) with that simulated from the X-ray crystal structure (bottom).

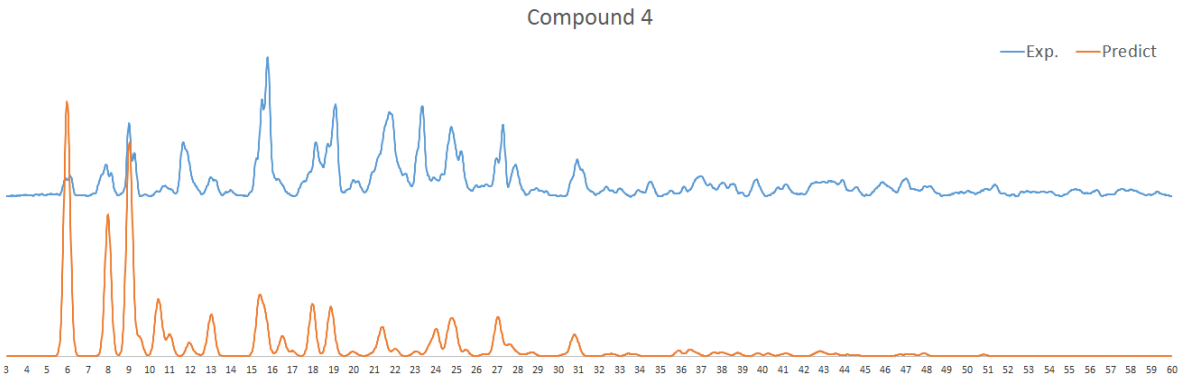

Figure S4. The PXRD pattern for $[Zn_2(mbdc\text{-}Me)_2(Hdpp)_2]\cdot DMF$ **4**, comparing the experimental pattern (top) with that simulated from the X-ray crystal structure (bottom).

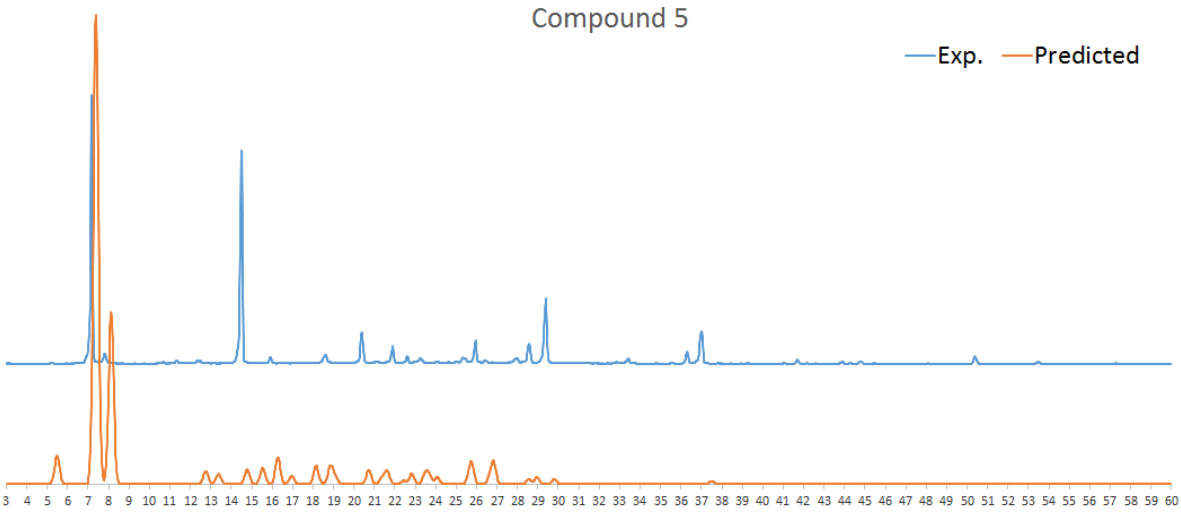

Figure S5. The PXRD pattern for $[Zn_2(2,6\text{-}ndc)_2(Hdpp)]\cdot DMF$, comparing the experimental pattern for a mixture of **5a** and **5b** (top) with that simulated from the X-ray crystal structure of **5b** (bottom).

4. Crystal structures

Details of the data collections, solutions and refinements for compounds **1-5** are given in Tables S1-3.

Table S1 – Crystallographic data for compounds **1**, **2a** and **2b**

Identification code	**1**	**2a**	**2b**
Empirical formula	$C_{96}H_{84}N_{20}O_{20}Zn_4$	$C_{49}H_{50}N_8O_{12}Zn_2$	$C_{112}H_{92}N_{20}O_{20}Zn_4$
Formula weight	2099.31	1073.71	2299.53
Temperature/K	150(2)	200.00(10)	150(2)
Crystal system	orthorhombic	tetragonal	triclinic
Space group	$P2_12_12_1$	$I4/mmm$	$P\bar{1}$
a/Å	16.5520(2)	21.7570(4)	18.532(2)
b/Å	18.8640(2)	21.7570(4)	20.3541(15)
c/Å	29.4330(3)	34.6535(11)	20.561(2)
α/°	90	90	116.099(8)
β/°	90	90	112.218(10)
γ/°	90	90	97.506(7)
U/Å^3	9190.07(17)	16403.8(8)	6022.4(11)
Z	4	8	2
ρ_{calc}/ g cm^{-3}	1.517	0.870	1.268
μ/mm^{-1}	1.116	1.075	0.858
F(000)	4320.0	4448.0	2368.0
Crystal size/ mm^3	0.35 × 0.3 × 0.28	0.212 × 0.173 × 0.042	0.1 × 0.08 × 0.08
Radiation	MoKα (λ = 0.71073)	CuKα (λ = 1.54184)	MoKα (λ = 0.71073)
2θ range for data collection/ °	7.046 to 55.01	7.684 to 140.112	5.992 to 43.932
Index ranges	$-20 \le h \le 21$, $-24 \le k \le 24$, $-38 \le l \le 38$	$-17 \le h \le 22$, $-16 \le k \le 26$, $-27 \le l \le 35$	$-19 \le h \le 16$, $-21 \le k \le 21$, $-21 \le l \le 21$
Reflections collected	125929	56809	24223
Independent reflections, R_{int}	20994, 0.0638	3216, 0.0540	13116, 0.1069
Data/restraints/parameters	20994/17/1307	3216/131/166	13116/86/414
Goodness–of–fit on F^2	1.061	1.704	0.978
Final $R1$, $wR2$ indexes [$I \ge 2\sigma(I)$]	0.0389, 0.0715	0.1169, 0.3989	0.1463, 0.3576
Final $R1$, $wR2$ indexes [all data]	0.0651, 0.0782	0.1381, 0.4342	0.2341, 0.4158
Largest diff. peak/hole / e Å^{-3}	0.28/–0.32	1.86/-1.13	1.95/–0.83
Flack parameter	0.488(9)	–	–

Table S2 – Crystallographic data for compounds **3** and **4**

Identification code	**3**	**4**
Empirical formula	$C_{24}H_{21}N_5O_5Zn$	$C_{47}H_{39}N_9O_9Zn_2$
Formula weight	524.83	1004.61
Temperature/K	150(2)	150(2)
Crystal system	orthorhombic	monoclinic
Space group	$P2_12_12_1$	$P2_1/c$
a/Å	10.1440(1)	10.040(6)
b/Å	13.9760(1)	29.598(17)
c/Å	16.1920(2)	17.153(11)
α/°	90	90
β/°	90	102.762(5)
γ/°	90	90
U/Å^3	2295.58(4)	4971(5)
Z	4	4
ρ_{calc}/ g cm^{-3}	1.519	1.342
μ/mm^{-1}	1.117	0.948
F(000)	1080.0	2064.0
Crystal size/ mm^3	0.5 × 0.35 × 0.1	0.04 × 0.03 × 0.02
Radiation	MoKα (λ = 0.71073)	Synchrotron (λ = 0.68890)
2θ range for data collection/ °	7.068 to 54.992	4.404 to 50
Index ranges	$-13 \le h \le 13$, $-18 \le k \le 18$, $-21 \le l \le 21$	$-12 \le h \le 12$, $-33 \le k \le 31$, $-21 \le l \le 21$
Reflections collected	44382	29660
Independent reflections, R_{int}	5253, 0.0685	8676, 0.0938
Data/restraints/parameters	5253/0/345	8676/191/648
Goodness–of–fit on F^2	1.052	1.061
Final $R1$, $wR2$ indexes [$I \ge 2\sigma(I)$]	0.0282, 0.0664	0.0740, 0.1986
Final $R1$, $wR2$ indexes [all data]	0.0317, 0.0679	0.0831, 0.2075
Largest diff. peak/hole / e Å^{-3}	0.26/–0.44	0.67/–0.96
Flack parameter	0.092(12)	–

Table S3 – Crystallographic data for compounds **5a** and **5b**

Identification code	**5a**	**5b**
Empirical formula	$C_{40}H_{29}N_5O_9Zn_2$	$C_{40}H_{29}N_5O_9Zn_2$
Formula weight	854.42	854.42
Temperature/K	150(2)	150.00(10)
Crystal system	triclinic	monoclinic
Space group	*P*–1	$P2_1/c$
a/Å	8.1920(2)	21.9269(10)
b/Å	16.4330(4)	23.8222(11)
c/Å	16.4440(4)	8.2020(2)
α/°	93.714(1)	90
β/°	99.822(1)	96.821(3)
γ/°	99.807(1)	90
U/Å^3	2139.30(9)	4254.0(3)
Z	2	4
ρ_{calc}/ g cm^{-3}	1.326	1.334
μ/mm^{-1}	1.177	1.184
F(000)	872.0	1744.0
Crystal size/ mm^3	0.2 × 0.13 × 0.08	0.41 × 0.27 × 0.19
Radiation	MoKα (λ = 0.71073)	Mo Kα (λ = 0.71073)
2θ range for data collection/ °	7.07 to 55.124	6.574 to 54.968
Index ranges	$-10 \le h \le 10$, $-21 \le k \le 21$, $-21 \le l \le 21$	$-28 \le h \le 28$, $-30 \le k \le 30$, $-10 \le l \le 10$
Reflections collected	42369	74335
Independent reflections, R_{int}	9831, 0.0719	9743, 0.0514
Data/restraints/parameters	9831/25/550	9743/0/551
Goodness–of–fit on F^2	1.041	1.030
Final *R*1, *wR*2 indexes [$I \ge 2\sigma(I)$]	0.0488, 0.1306	0.0677, 0.1641
Final *R*1, *wR*2 indexes [all data]	0.0941, 0.1493	0.0943, 0.1810
Largest diff. peak/hole / e Å^{-3}	0.40/–0.41	1.78/–0.82
Flack parameter	–	–

Points of interest from the data collections and refinements are detailed below.

For **1**, in the DMF molecules containing N(19), all atoms except for the nitrogen, are disordered over two sites in a 65:35 ratio. Some distance restraints were added to aid refinement in the final least squares. The nitrogen bound hydrogen atoms in the Hdpp ligands were located but ultimately included at calculated positions, although the U_{iso} values were refined. The diffraction data suggested racemic twinning which was accounted for in the refinement.

Attaining a reasonable model in the case of **2a** was fraught with difficulty. Integration of the raw images, using the default settings, in the CrysAlisPro software offered a tetragonal *P*-type Bravais lattice. Efforts to assign an appropriate space group were not straightforward, with no consistency achievable between the space group determination algorithms in Olex[2], WinGX, SHELXL, superflip solution routines or human determination of the absences.

Ultimately, however, a solution was brokered in space group $P4_2/mnm$ with similar unit cell parameters to those reported here. The accompanying R_{int} was an entirely credible value of 0.0638, but the *R*1 value was in the region of just below 20% and there were violations of the *n*-glide absence condition. These observations combined to suggest that something was clearly wrong and, at minimum, twinning of the sample should be explored. Despite extensive efforts to solve the structure in twinned and untwinned tetragonal, orthorhombic, monoclinic and triclinic settings, none of these resulted in a model improvement over that which had been obtained in space group $P4_2/mnm$. It became clear that there was a weakness in the intensities of those data which would be systematically absent were the Bravais lattice an *I*-type. Thus, it was a case of returning to reintegrate the data with a higher spike threshold at the outset. The resultant dataset emerged as tetragonal *I*, the highest possible suggested space group symmetry was $I4/mmm$, and this ultimately afforded the model presented herein with a more sensible set of residuals that have been previously obtained from the model refined in the tetragonal *P*-type lattice.

While this is the optimal refinement that could be obtained from these data, the results are presented with caveats. On the plus side, the architecture of the framework (similar to that obtained in the $P4_2/mnm$ model) is unambiguous. Clearly, there were deficiencies in the original data which may point to a more complicated twinning type being present than was possible to resolve. (While lower symmetry *I*-type tetragonal, orthorhombic and monoclinic space groups were also explored, they offered (where a solution was possible) no improvement over achieved that in $I4/mmm$). The result of the superflip routine implemented in their WinGX software, which is not biased by space group knowledge, did however support the space group choice presented here.

With respect to the structure itself, the asymmetric unit comprises half of the zinc centre, half of an ndc ligand, half of a Hdpp ligand and some diffuse solvent. With the exception of C(2), the aromatic carbon atoms in the dicarboxylate ligand were modelled for disorder over two sites in a 50:50 ratio. The ADPs associated with these fractional occupancy carbons suggest some waving of the naphthalene core about the C(1)-C(2) axis. C(5)/(5A) and C(6)/(6A) were refined isotropically as a result, and because of the electron density smearing in this region, several C–C distance restraints were also included in the model. Indeed, there was some evidence for additional disorder of C(5)/(5A) and C(6)/C(6A) on the opposing side of the central phenyl group (i.e. attached to C(3)/C(3A) rather than C(2)/C(2A)), but this was not at a level that could be modelled with any credibility. Crystallographically induced disorder

about a mirror plane was also prevalent in the Hdpp moiety, with atoms N(1), and C(7)-C(13) present at half site occupancy. Additional disorder (50:50 ratio) was also counted for in the case of N(2). In order to assist refinement, the pyridyl ring was treated as a rigid hexagon, while distance restraints were employed for the pyrazole ring and ADP restraints were included throughout. The pyrazole hydrogen was included as being disordered in equal measure over the nitrogen content of said 5-membered ring.

Diffuse solvent in the pores was treated using the solvent mask algorithm in Olex^2 and an allowance of one molecule of DMF per asymmetric unit has been made for same, in the formula presented here.

While the refinement of **2b** converged well in terms of shift/ESD values, this was only achieved with the addition of distance and planarity restraints as well as displacement parameter constraints. These shortcomings in the model reflect a sharp decline of diffraction intensity by this material after a resolution of 1.25° which, in turn, signals the mediocre crystal quality and some twinning. A parallel refinement was pursued, based on integration of the raw data to take account for twinning of 174° about the 0 0 1 reciprocal axis. However, this afforded no advance in terms of convergence, and the contribution for the second component refined to approximately 8%. Hence, this refinement was abandoned in favour of what is presented here.

The worst affected regions concern the carboxylate ligands, largely perhaps because the resolution of the data is not good. The high angle data were diffuse at best. Only the zinc atoms were treated anisotropically due to the data quality. An analysis of the void space has resulted in one molecule of DMF being included in the formula as presented, per zinc centre. SQUEEZE was not applied to the data, as the quality of same hampered the usual employment of this algorithm in a manner that enhances the refinement. Hydrogen atoms attached to the pyrazole moieties are largely dictated by the opportunity for hydrogen-bonding in the gross structure. Despite shortcomings, what we have here is an unambiguous assignment of the interpenetrated framework in this compound. We do not intend to make any claims about the individual metric data presented herein.

In the structure of **4**, atoms C(11A)-C(14A) and C(16) exhibit disorder in a 75:25 ratio. Restraints were placed on ADPs of atoms with less than 100% occupancy. An ordered DMF molecule is present in the asymmetric unit, with half occupancy, and this could be modelled with some confidence. However, residual electron density suggested additional diffuse solvent content which was treated with PLATON SQUEEZE. This has been included here as an additional half molecule of DMF per asymmetric unit, based on the pre-SQUEEZE difference Fourier map, and the PLATON calculations.

The solvent included within the lattice of **5a** is diffuse and is estimated as one DMF per asymmetric unit. This estimate is based on the pre-SQUEEZE evident electron density, in combination with the SQUEEZE output. The hydrogen atom attached to either N(3) or N(4) could not be located with any credibility, and hence was omitted from the refinement. The phenyl carbons in the two crystallographically independent ligand halves are subject to 50:50 disorder, which was readily modelled by employing minimal restraints to assist convergence.

The solvent included in the lattice of **5b** is also diffuse and is estimated as one DMF per asymmetric unit. This estimate is based on the electron density evident pre-SQUEEZE, in combination with the output after applying this algorithm. The hydrogen which could have been attached to either N(3) or N(4) was ultimately included for the latter based on analysis of

U_{iso} values for trials involving both nitrogen atoms. The phenyl carbons in the two crystallographically independent ligand halves are subject to 50:50 disorder in one case and 65:35 disorder in the other. This disorder was readily modelled by employing minimal restraints to assist convergence.

Crystals of **2b** were observed to undergo a morphological change when removed from their reaction medium in air as can be seen in Figure S6.

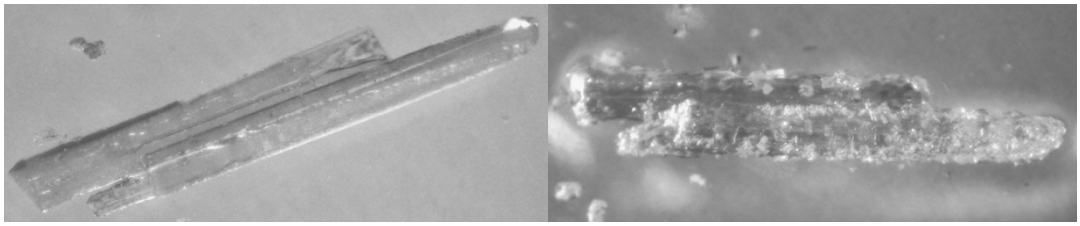

Figure S6. The colourless crystals of [Zn(1,4-ndc)(Hdpp)] **2b**: (left) as-synthesised and (right) after 10 min left out of the mother liquor.

5. References

S1. W. Kraus and G. Nolze, *J. Appl. Cryst.*, 1996, **29**, 301.

S2. I. J. Bruno, J. C. Cole, P. R. Edgington, M. Kessler, C. F. Macrae, P. McCabe, J. Pearson and R. Taylor, *Acta Crystallogr., Sect. B*, 2002, **58**, 389.